The Astrophysical Journal, 689:53–58, 2008 December 10

A CHARACTERISTIC PLANETARY FEATURE IN DOUBLE-PEAKED, HIGH-MAGNIFICATION MICROLENSING EVENTS

Cheongho Han[1] and B. Scott Gaudi[2]
Received 2008 May 8; accepted 2008 August 4

ABSTRACT

A significant fraction of microlensing planets have been discovered in high-magnification events, and a significant fraction of these events exhibit a double-peak structure at their peak. However, very wide or very close binaries can also produce double-peaked high-magnification events, with the same gross properties as those produced by planets. Traditionally, distinguishing between these two interpretations has relied on detailed modeling, which is both time-consuming and generally does not provide insight into the observable properties that allow discrimination between these two classes of models. We study the morphologies of these two classes of double-peaked, high-magnification events and identify a simple diagnostic that can be used to immediately distinguish between perturbations caused by planetary and binary companions, without detailed modeling. This diagnostic is based on the difference in the shape of the interpeak region of the light curves. The shape is smooth and concave for binary lensing, while it tends to be either boxy or convex for planetary lensing. In planetary lensing this interpeak morphology is due to the small, weak cusp of the planetary central caustic located between the two stronger cusps. We apply this diagnostic to five observed double-peaked, high-magnification events to infer their underlying nature. A corollary of our study is that good coverage of the interpeak region of double-peaked, high-magnification events is likely to be important for their unique interpretation.

Subject heading: gravitational lensing

1. INTRODUCTION

Microlensing has emerged as an important method of discovering extrasolar planets. Since the first discovery in 2004, six microlensing planets have been reported (Bond et al. 2004; Udalski et al. 2005; Beaulieu et al. 2006; Gould et al. 2006; Gaudi et al. 2007). The detection rate is rapidly increasing, and six additional planet candidates were detected during the 2007 season alone (Gould 2008). In contrast to the radial velocity and transit methods, which are most sensitive to planets that orbit close to their parent star, the sensitivity of the microlensing method peaks in the cool, outer regions of planetary systems beyond the "snow line" (Gould & Loeb 1992; see also Gaudi 2008). Furthermore, the sensitivity of the microlensing method extends to very low mass planets (Bennett & Rhie 1996). Thus, microlensing is sensitive to planets with physical properties that are very different from those discovered by other methods, and the sample of microlensing planets includes notable planets such as the most distant, the coldest, and the lowest mass planets detected to date. In addition, the recently reported multiple-planet system OGLE-2006-BLG-109Lb,c (Gaudi et al. 2007) is also noteworthy in that the planet masses and locations relative to the snow line are similar to those of Jupiter and Saturn.

Microlensing planet searches are currently conducted using a combination of survey and follow-up observations. The primary microlensing events, caused by stars in the Galactic bulge or foreground disk, are found by survey observations (Soszyński et al. 2001; Bond et al. 2001), which maximize the event rate by monitoring a large area of the Galactic bulge on a roughly nightly basis. These data are analyzed real-time, thereby making it possible to issue alerts of ongoing events in the early stage of lensing magnification. Follow-up observations (Yoo et al. 2004; Cassan et al. 2004) are focused on these alerted events in order to detect the short-lived perturbations to the light curves of the host stars that are the signals of planetary companions to these stars. However, the limited number of telescopes available for follow-up restricts the number of events that can be followed at any given time. Thus, priority is given to those events that will maximize the planetary detection probability. Currently, the highest priority is given to high-magnification events. There are several reasons for this. First, these events have high intrinsic planet detection efficiency because the source trajectories of these events always pass close to the perturbation region around the central caustic induced by the planet (Griest & Safizadeh 1998). Second, follow-up observations can be prepared in advance because the time of perturbation typically occurs near the peak of the event, which can be predicted reasonably well from data taken on the rise to the peak. Third, the enhanced brightness of the highly magnified source near the event peak allows for precision photometry, which is essential for the proper characterization of the planetary perturbation. In addition, these bright event peaks can be observed using small-aperture telescopes, which are much more numerous, thus enabling continuous and frequent monitoring, which is also essential for proper characterization. As a result, four (OGLE-2005-BLG-071Lb, OGLE-2005-BLG-169Lb, and OGLE-2006-BLG-109Lb,c) of the six reported microlensing planets were detected through the channel of high-magnification events.

A common morphology of perturbed high-magnification events is a double-horned, or double-peaked, structure at the peak of the light curve. A double-peaked morphology at the peak of a high-magnification event can be produced in two very different ways. The first is when the source approaches the blunt, back end of the asymmetric, wedge-shaped, central caustic of a planetary companion at an angle of $\sim 90^\circ$ from the planet/star axis. The second arises when the source approaches the symmetric astroid-shaped caustic of a very wide or very close binary at an angle of $\sim 45^\circ$ from the binary axis. The light curves of these two types

[1] Program of Brain Korea 21, Physics Department, Chungbuk National University, Cheongju 361-763, Korea; cheongho@astroph.chungbuk.ac.kr.
[2] Department of Astronomy, Ohio State University, 140 West 18th Avenue, Columbus, OH 43210-1173; gaudi@astronomy.ohio-state.edu.

of events are approximately degenerate in the sense that one can find a value of the shear (for a wide binary lens) or quadrupole moment (for a close binary lens) such that the peak heights and time between the peaks are roughly the same as for the planetary case. Fortunately, as has been demonstrated empirically (Albrow et al. 2002), they are not perfectly degenerate; thus with sufficient data quality and quantity it is possible to determine whether a light curve is due to a planet or a binary. Distinguishing between the planetary or close/wide binary interpretations of an observed double-peaked high-magnification event has heretofore required detailed modeling (e.g., Albrow et al. 2002).

In this paper, we study the morphology of double-peaked, high-magnification events and identify a diagnostic feature of the interpeak region of these light curves that can be used to immediately distinguish between the planetary and binary interpretations. Specifically, the interpeak region of planetary events is typically boxy or convex, whereas it is smooth and concave for close or wide binary lenses. We provide the physical basis for this difference in the morphology, which is related to the existence of a third, weak cusp in the central caustic of planetary lens, which is absent in the close/wide binary case. While detailed modeling of observed events is ultimately required to derive precise values of the underlying physical parameters, this approach is time-consuming. This diagnostic can be used to quickly identify those events that are most likely caused by planetary companions and thus permit efficient allocation of limited modeling resources. Furthermore, our study provides some insight into the kinds of observations that are needed to discriminate between these two classes of models. This can aid in the planning of observations and, if this diagnostic is applied to events real-time, can inform decisions about which events to follow given limited observational resources.

2. LENSING PROPERTIES

For a binary lens, the mapping between the lens plane and source plane can be expressed as

$$\zeta = z - \frac{m_1/M}{\bar{z} - \bar{z}_{L,1}} - \frac{m_2/M}{\bar{z} - \bar{z}_{L,2}}, \tag{1}$$

where $\zeta = \xi + i\eta$, $z_{L,j} = z_{L,j} + iy_{L,j}$, and $z = x + iy$ are the complex angular positions of the source, lens, and image, respectively, $\bar{z}$ denotes the complex conjugate of z, $j = 1$ and 2 denote the primary and companion, respectively, m_j are the masses of the individual lens components, and $M = m_1 + m_2$ is the total mass (Witt 1990). Here all angles are normalized to the Einstein radius corresponding to the total mass of the lens system

$$\theta_{\rm E} = \left[\frac{4GM}{c^2}\left(\frac{1}{D_L} - \frac{1}{D_S}\right)\right]^{1/2}, \tag{2}$$

where D_L and D_S are the distances to the lens and source, respectively. For a binary lens, there exist three or five images depending on the source position with respect to the positions of the lens components. The magnification of each image is the ratio between the areas of the image and source. This corresponds to the reciprocal of the determinant of the Jacobian of the lens mapping evaluated at the image position, i.e.,

$$A_i = \left|\left(1 - \frac{\partial\zeta}{\partial\bar{z}}\frac{\overline{\partial\zeta}}{\partial\bar{z}}\right)^{-1}_{z=z_i}\right|. \tag{3}$$

Then the total magnification is the sum of the magnifications of the individual images, $A = \sum_i A_i$.

An important characteristic of binary lensing is the existence of caustics. They represent the set of source positions at which the magnification of a point source becomes infinite (i.e., where the determinant of the Jacobian is zero) and mark the boundaries of the region in the source position where the number of images differs by two. For a binary lens, the caustics form one, two, or three closed curves, interior to which there are five images. Each set of caustics is composed of smooth, concave curves that are fold singularities, which meet at points that are higher order, cusp singularities.

2.1. *Planetary Lensing*

Planetary lenses correspond to an extreme case of the binary lens where the mass of one of the lenses is much smaller than the other. In this case, the lens equation can be rewritten in a somewhat more intuitive form,

$$\zeta = z - \frac{1}{\bar{z}} - \frac{q}{\bar{z} - \bar{z}_p}, \tag{4}$$

where the angular coordinates are centered at the position of the planet-hosting star, z_p represents the location of the planet, q is the planet/star mass ratio, and the angular positions are now normalized to the Einstein radius of the primary mass. In the case of $q \ll 1$, the analysis of the lensing behavior is amenable to a perturbative approach, which yields considerable insight into the behavior of the caustics and light curves as a function of the planetary parameters (Dominik 1999; Bozza 1999; Asada 2002; An 2005).

For the planetary case, unless $|z_p| \sim 1$, there exist two sets of disconnected caustics. One set, which can consist of one or two closed caustic curves, is located away from the host star. This set is typically referred to as the planetary caustic (or caustics). The location of the planetary caustic relative to the source trajectory depends on the separation between the planet and star, as well as the angle between the planet/star axis and the direction of motion of the source. Thus, perturbations due to planetary caustics are not predictable.

In contrast to the planetary caustic or caustics, the other caustic is always located close to the host star and so is known as the central caustic. Thus, central caustic perturbations always occur at the peak of high-magnification events. The central caustic has a wedgelike shape with *four* cusps (see Fig. 1). One cusp is located on the star-planet axis and corresponds to the point of the wedge. This cusp is strong, in the sense that light curves from source trajectories that pass reasonably close to such a cusp will exhibit strong deviations from the single-lens expectation. Two of the cusps are located off the axis on the opposite side of the caustic and define the "blunt" end of the wedge-shaped caustic. These two cusps are also strong. Between these cusps is a region of significant demagnification relative to the single-lens expectation. The fourth cusp, which is located between these cusps on the planet-star axis, is weak, in the sense that it creates relatively weak positive deviations (see Fig. 1). Because of this wedge-shaped geometry, central caustic perturbations typically occur when the source passes close to either the point or the blunt end of the wedge on a trajectory that is approximately perpendicular to the planet/star axis. In the case that it passes the blunt end, the resulting light curve is double-peaked. In fact, both of the planetary microlensing events arising from central caustic perturbations have been double-peaked, suggesting that this class of events might be quite common.

The size of the central caustic depends on both the star-planet separation and planet/star mass ratio. When the size is measured

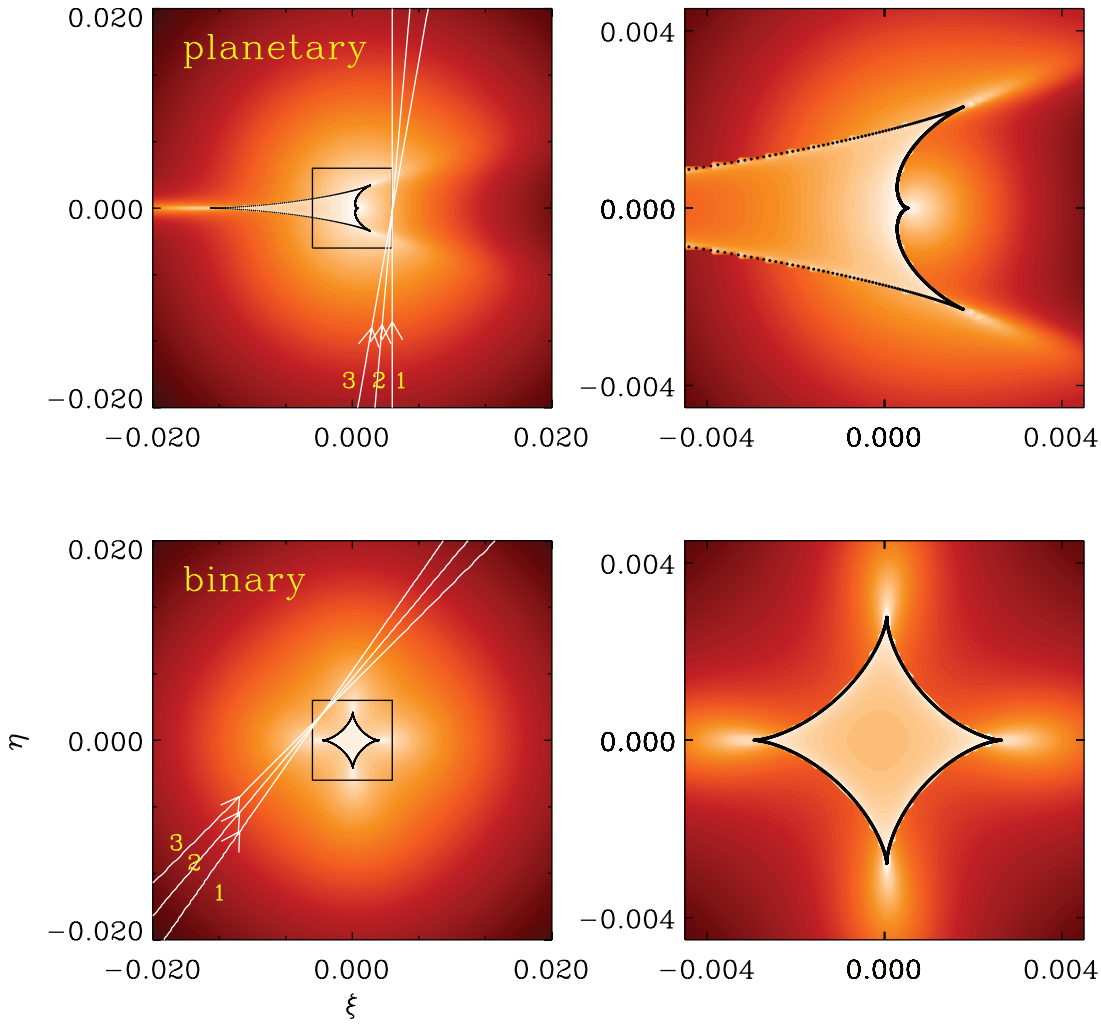

FIG. 1.—Magnification map as a function of the angular position of the source for a planet/star (*upper panels*) and a wide binary-lens (*lower panels*) system. The map for the planetary system shows a small region around the planet-hosting star. Angles are in units of the Einstein radius of the planet-hosting star. The planet is located to the left with a separation corresponding to 1.3 times of the star's Einstein radius, and the planet/star mass ratio is 10^{-3}. The map of the binary system shows the region in the vicinity of the primary lens of the two, equal-mass, binary-lens components. Angles are in units of the angular Einstein radius of the primary lens. The other, secondary lens component is located to the left with a separation corresponding to 26.9 times the Einstein radius of one component. In all panels, the coordinates are aligned such that ξ and η axes are parallel with and normal to the line connecting the two lens components, respectively. The closed figures drawn in thick black curves represent the caustics. The color scale is drawn such that the brighter tone represents the region of higher magnification. The straight lines with arrows show three different source trajectories leading to the double-peaked light curves presented in Fig. 2. The maps on the right panels show blowups of the regions enclosed by the boxes in the left panels.

as the separation between the two on-axis cusps, it is related to the separation and mass ratio by

$$\Delta\xi_c \simeq \frac{4q}{(s - s^{-1})^2}, \tag{5}$$

where the separation s is expressed in units of the Einstein radius. Unlike the size, which depends on both s and q, for $q \ll 1$ the shape of the caustic is solely dependent on s and it becomes more elongated as $s \rightarrow 1$. For a given mass ratio, a pair of central caustics with separations s and s^{-1} are identical to first order in q. For more details about the properties of central caustics, see Chung et al. (2005).

In the upper panels of Figure 1, we present the central caustic of an example planetary lens system and the magnification pattern around the caustic. The planet has a mass ratio $q = 10^{-3}$, and it is located on the left side of the host star with a separation $s = 1.3$. The coordinates are centered at the location of the host star, and the axes are aligned such that the ξ and η axes are parallel with and perpendicular to the star-planet axis, respectively. All angular positions are normalized in units of the Einstein radius corresponding to the mass of the planet-hosting star. The color scale is drawn such that the brighter tone represents the region of higher magnification. The straight lines with arrows are example source trajectories producing double-peaked events where the light curves of the resulting events are presented in Figure 2 (*blue curves*). The source trajectories have a common impact parameter from the primary star, but the angles with respect to the star-planet axis (source trajectory angle α) are different. For the planetary case, the two peaks have a similar height when the source trajectory angle is $\alpha \sim 90^\circ$, and the difference in heights increases as the angle deviates from this angle. The map in the upper right panel shows a blowup of the region enclosed by a box in the upper left map.

2.2. *Wide/Close Binary Lensing*

In the limiting case of a binary lens where the projected separation between the lens components is much larger than the Einstein radius ($s \gg 1.0$), the lensing behavior in the vicinity of

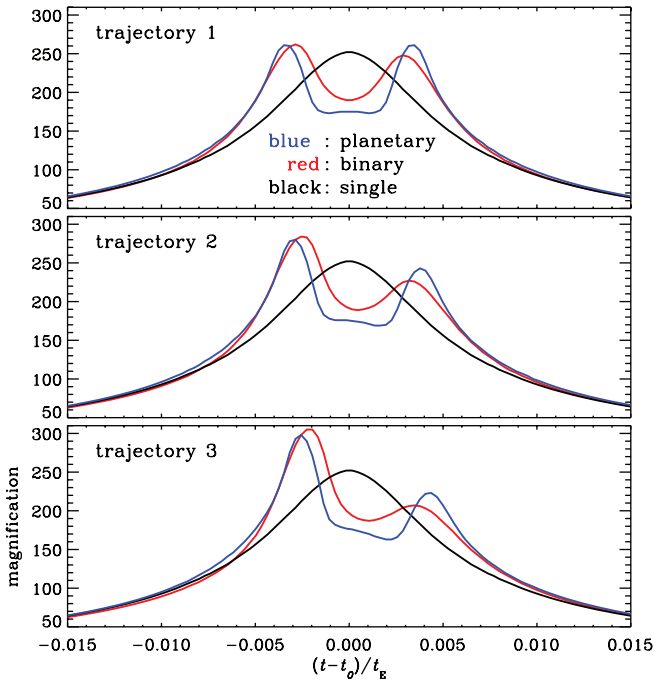

FIG. 2.—Examples of double-peaked, high-magnification light curves. The geometry of the lens systems and the source trajectories responsible for the light curves are presented in Fig. 1. In each panel, blue and red curves are the light curves for the planetary and binary events, respectively, whereas the black curve is the light curve for a single lens with the same mass as the primary lens (i.e., no planetary or binary companion). The time is relative to t_0, the time of closest approach to the origin of the lens system, and normalized to t_E, the Einstein timescale of the primary lens.

one of the lens components (the primary) can be approximated by a Chang-Refsdal lens (Chang & Refsdal 1979, 1984; Dominik 1999), i.e.,

$$\hat{\zeta} = \hat{z} - \frac{1}{\hat{z}} + \gamma\hat{z}, \tag{6}$$

where the notations with a "hat" represent angular scales normalized by the Einstein radius of the primary. The quantity γ represents the shear induced by the other binary component (companion), and it is related to the lens parameters by

$$\gamma = \frac{q}{\hat{s}^2}, \tag{7}$$

where $q = m_2/m_1$ is the companion/primary mass ratio, m_1 and m_2 are the masses of the primary and companion, respectively, and $\hat{s}$ is the separation between the primary and the companion in units of the Einstein radius of the primary, which is related to the separation in units of the Einstein radius of the total mass of the binary by $\hat{s} = (1+q)^{1/2}s$.

The shear exerted by the companion results in the formation of a small caustic near the location of the primary lens. In the Chang-Refsdal limit, the caustic has a shape of hypocycloid with four cusps (an astroid) regardless of the binary separation and mass ratio. Two of the cusps are located on the binary-lens axis, and the other two are along a line perpendicular to the axis. All of these cusps are of equal strength. Thus, a source trajectory that passes close to the caustic on a trajectory with an orientation of $\sim 45^\circ$ with respect to the binary axis will produce a double-peak event with roughly equal peak heights. The size of the caustic as measured by the separation between the two on-axis cusps is

$$\Delta\xi_c \simeq 4\gamma, \tag{8}$$

and thus $\Delta\xi_c \propto q$ and $\Delta\xi_c \propto \hat{s}^{-2}$.

For a close binary with $s \ll 1.0$, the caustic and the magnification pattern around it are approximately identical to those of the wide binary with a separation of s^{-1}, except that the caustic is located at the center of mass of the binary. In this case, the size of the caustic is set by the quadrupole moment of the binary.

In the lower left panel of Figure 1, we present the magnification pattern in the vicinity of the primary of a wide binary lens. The companion is located on the left side with a separation of $\hat{s} = 26.9$, and the companion/primary mass ratio is 1.0. In the map, we also mark several example source trajectories resulting in double-peaked high-magnification events, where the light curves are presented in Figure 2 (*red curves*). These trajectories have $\alpha \sim 45^\circ$, and thus the two peaks have a similar height. The notations are the same as those of the maps of the planetary lens.

3. DIFFERENCE IN MAGNIFICATION PATTERN

The perturbations from the single-lens form exhibited in double-peaked high-magnification events can be characterized by three gross observables: the height of each peak and the time between the two peaks. Given an observed double-peaked, high-magnification event, it is always possible to find a planetary or binary-lens model that can reproduce these observables. In particular, these three observables can be matched by varying the following three parameters: (1) the angle of the source trajectory relative to the binary lens axis, which sets the relative peak heights, (2) the impact parameter from the primary lens,[3] which sets the average height of the two peaks, and (3) either the shear (in the case of a wide binary), the quadrupole moment (in the case of a close binary), or the parameter combination $q(s - s^{-1})^{-2}$ (in the case of the planetary lens), which set the size of the caustic and so the time between the peaks.

Although it is possible to match these three gross observables with either a planetary or wide/close binary lens, the morphology of these two classes of double-peaked, high-magnification events are not identical, as illustrated in Figure 2. The most noticeable difference arises in the shape of the interpeak, trough region. In the case of a close/wide binary lens, this region has a smooth, rounded, concave shape. On the other hand, in the case of the planetary lens curve, this region has a boxy, slightly convex morphology.

The morphology of the interpeak trough region in the planetary case is caused by the existence of the fourth cusp in the central caustic located in between the two stronger cusps (see the blowup of the planetary central caustic in the upper right panel of Fig. 1). The general pattern of magnification around a caustic is a lobe of positive perturbation in the region immediately surrounding the cusp, flanked on the side of the cusp by a more extended region of relative demagnification. For the planetary case, the weak fourth cusp results in either a boxy intertrough region, or even a slight convexity, caused by the lobe of positive perturbation associated with the weak cusp "filling in" the trough created by the two neighboring, stronger cusps. Since the cusp is weak, this bump is generally weak, but its effect on the morphology of the light curve is generally not negligible. For close/wide binary

[3] It is not strictly true that it is possible to vary the impact parameter arbitrarily, as this parameter is constrained by the light-curve data away from the peak. However, for high-magnification events in the usual highly blended case, the impact parameter is poorly constrained, and thus our discussion is approximately correct.

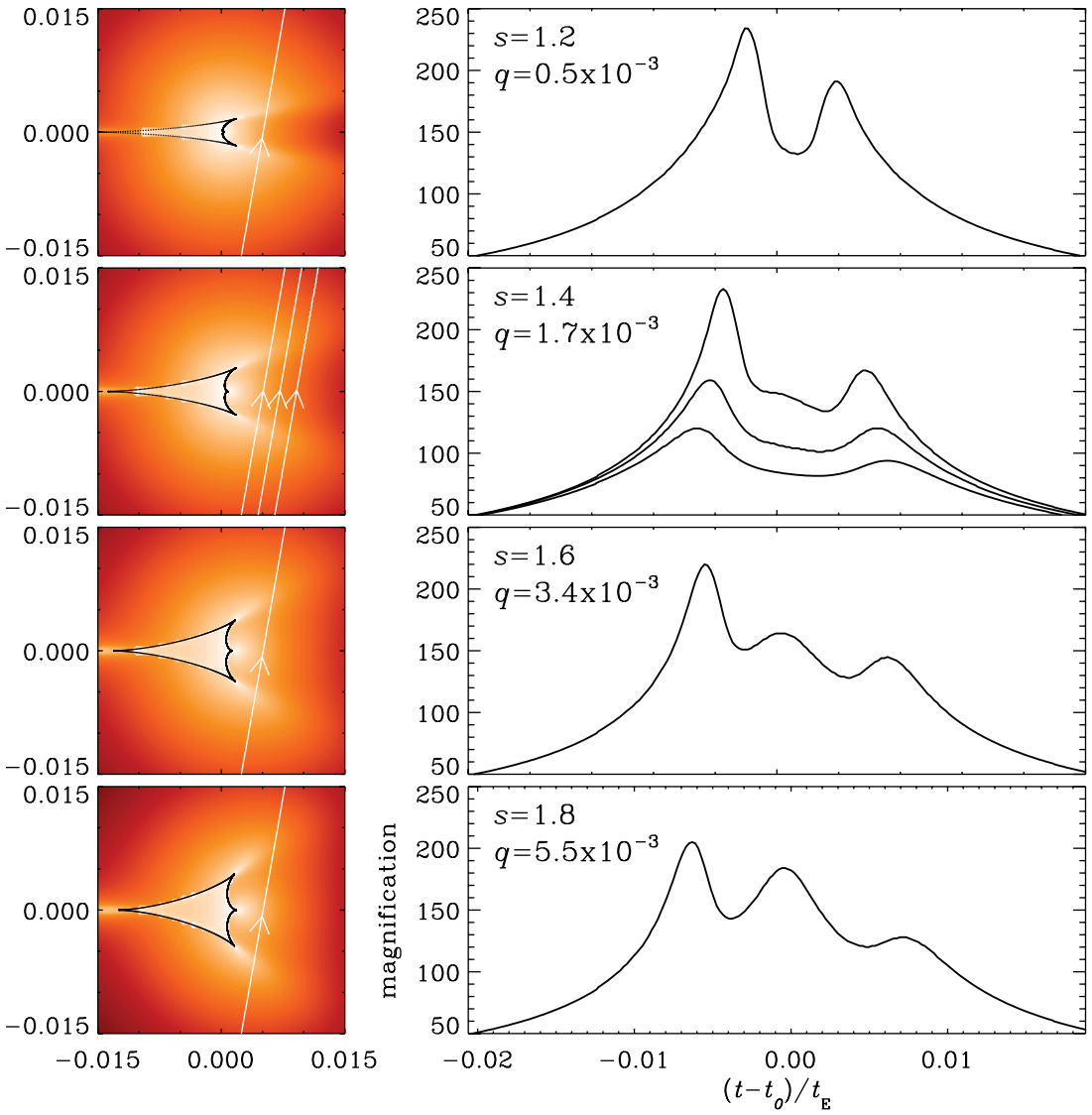

FIG. 3.—Variation of the interpeak morphology of double-peaked, high-magnification planetary microlensing events. The left panels show the magnification patterns around central caustics of various shapes. In each panel, the white lines indicate example trajectories, with the corresponding light curves shown in the right panels. In the second row, several trajectories are shown to illustrate the effect of the varying the impact parameter of the source trajectory on the interpeak morphology. Notations for the magnification pattern maps are the same as in Fig. 1. The values marked in each panel represent the star-planet separation in units of the Einstein radius (s) and the planet/star mass ratio (q).

lenses, on the other hand, there is no weak middle cusp. Thus, the interpeak morphology for a binary lens caustic is characterized by the double peaks that occur when the source approaches the strong cusps of the astroid Chang-Refsdal caustic, and a smooth, concave interpeak trough that occurs as the source passes through the negative perturbation region between the two cusps.

The impact of the weak middle cusp on the planetary lensing light-curve morphology varies depending on the underlying parameters. Two factors affect the shape of the feature. The first is the overall shape of the central caustic. This can be seen in Figure 3, where we present magnification patterns around central caustics of various shapes, as well as example light curves. In order to isolate the effect of the caustic shape on the morphology, we have adjusted the parameters so that the caustics have a similar size [i.e., so that the parameter combination $q(s - s^{-1})^{-2}$ is constant]. The shape of the caustic depends on the star-planet separation s, and thus the shape of the interpeak feature depends on the planetary separation. The variation is such that the cusp responsible for the interpeak feature is stronger, and thus the interpeak feature is more prominent for a planet located farther from the Einstein radius of the central star. The other factor that affects the shape of the interpeak feature is the impact parameter of the source trajectory. As the source trajectory passes closer to the weak cusp, the resulting feature becomes more obvious. The variation of the interpeak feature with the impact parameter is shown in the second set of panels of Figure 3.

We note that although the interpeak region shows the most obvious morphological differences between the close/wide binary and planetary light curves, there are other, somewhat more subtle differences that may also be used to distinguish between these two interpretations. In particular, the detailed shapes of the peaks appear to differ. In the planetary case, the lobes of high magnification due to the strong cusps are asymmetric about the symmetry axes of the cusps, whereas for the binary-lens case the magnification patterns near the cusps are nearly perfectly symmetric about the symmetry axes. Thus, even in the case of a poorly sampled interpeak region, or when $s \rightarrow 1$ in the planetary lens case such that the middle cusp is very weak, detailed information

about the shape of the peaks will allow one to distinguish between the two models.

An important corollary to our study is that one expects that high-magnification, double-peaked events in which the interpeak region is poorly sampled to be subject to more severe degeneracies, such that the span of allowed models is larger. Thus, good coverage of the interpeak region is likely to be important for the unique interpretation of these events.

4. APPLICATION TO OBSERVED EVENTS

The diagnostic feature we have identified is useful as it can be used to distinguish between planetary and close/wide binary interpretations of observed events, without the need for detailed fitting. Thus, it can be used to quickly identify those events that are most likely due to planetary companions. Motivated by this, we apply our diagnostic to five high-magnification, double-peaked events with reasonably well-covered peaks.[4] For two of these events, MACHO 99-BLG-47 (Albrow et al. 2002) and OGLE-2005-BLG-071 (Udalski et al. 2005; Dong et al. 2008), detailed modeling has already been done. Three additional events were observed during the 2007 lensing season, for which detailed modeling has not been reported. These events are OGLE-2007-BLG-349/MOA-2007-BLG-379, OGLE-2007-BLG-514, and OGLE-2007-BLG-137/MOA-2007-BLG-091.

1. *MACHO 99-BLG-47*.—This is the first published high-magnification event with two well-resolved peaks. The trough between the two peaks of this event exhibits a smooth concave shape, suggesting that the lens is a wide/close binary and not a planetary system. The large difference between the heights of the two peaks implies that the source trajectory angle is considerably different from 45°. This diagnostic matches the results from the detailed analysis of the event conducted by Albrow et al. (2002). In this model, the source trajectory angle was estimated to be $\alpha \sim 25^\circ$.

2. *OGLE-2005-BLG-071*.—The interpeak trough of this event exhibits a prominent convex feature, implying that the perturbation is caused by a planet. In addition, the two peaks are of almost equal height, implying that the source passes nearly perpendicular to the binary axis. This diagnostic matches the results obtained from the detailed modeling conducted by Udalski et al. (2005) and Dong et al. (2008).

3. *OGLE-2007-BLG-349/MOA-2007-BLG-379*.—This event was detected during the 2007 season,[5] and its peak was densely covered by follow-up observations. The two peaks have moderately different heights, and the trough between the peaks has a linear structure. These characteristics are similar to the planetary lensing light curve presented in the middle panel of Figure 2, except with the direction of time reversed. Our diagnostic would therefore indicate that this event is caused by a planet with a source trajectory angle somewhat different from $\alpha = 90^\circ$.

4. *OGLE-2007-BLG-514*.—This is another double-peaked, high-magnification event observed during the 2007 season (see footnote 5). The interpeak trough shows a smooth concave shape, and thus we diagnose that the lens is a either wide or close binary and not a planetary system. The heights of the two peaks are similar, and thus the source trajectory angle is close to $\alpha = 45^\circ$.

5. *OGLE-2007-BLG-137/MOA-2007-BLG-091*.—The apparent magnification of this double-peaked event is only a modest $\sim$10, although the true magnification could be substantially higher if it is highly blended (see footnote 5). The interpeak trough is not well covered, but the data in this region appear to show a relatively sharp change in the slope of the magnification, perhaps followed by a linear rise. This morphology is indicative of a planetary (or at least low mass ratio) companion. The heights of the two peaks are quite different, implying a source trajectory angle significantly different from $\alpha = 90^\circ$, assuming that the event is due to a low mass-ratio companion.

5. CONCLUSION

We have investigated the morphology of double-peaked, high-magnification events, which can be produced by two very different classes of models: planetary lenses in which the source trajectory passes close to the back end of the wedge-shaped central caustic, and very wide or very close binary lenses in which the source passes close to two of the cusps of a Chang-Refsdal caustic. From a comparison of the morphology of the light curves produced by these two classes of models, we have identified a diagnostic that can be used to immediately distinguish between perturbations produced by a planet from those produced by a binary companion. This diagnostic is based on the difference in the shape of the interpeak region of the light curve. For binary lensing, the shape is smooth and concave, whereas for planetary lensing, the shape is boxy or convex. The morphology of the interpeak region of planetary lensing events is due to the existence of a weak cusp located between the two stronger cusps. Finally, we applied this diagnostic to five observed double-peaked, high-magnification events.

This work was supported by the Science Research Center (SRC) program. We would like to thank A. Gould for providing light curves of the events observed by the MicroFUN collaboration during the 2007 season.

[4] We do not consider those events that are technically double-peaked, high-magnification events but are clearly not produced by the two classes of models we have considered in this paper. An example is MOA-2002-BLG-33, which has a maximum magnification of $\sim$450 and exhibits a double-peaked morphology, but is clearly caused by a geometry in which the source trajectory crosses a caustic with a size of order the source size (Abe et al. 2003).

[5] See http://ogle.astrouw.edu.pl/ogle3/ews/ews.html and https://it019909.massey.ac.nz/moa/.

REFERENCES

Abe, F., et al. 2003, A&A, 411, L493
Albrow, M. D., et al. 2002, ApJ, 572, 1031
An, J. H. 2005, MNRAS, 356, 1409
Asada, H. 2002, ApJ, 573, 825
Beaulieu, J. P., et al. 2006, Nature, 439, 437
Bennett, D. P., & Rhie, S. H. 1996, ApJ, 472, 660
Bond, I. A., et al. 2001, MNRAS, 327, 868
———. 2004, ApJ, 606, L155
Bozza, V. 1999, A&A, 348, 311
Cassan, A., et al. 2004, A&A, 419, L1
Chang, K., & Refsdal, S. 1979, Nature, 282, 561
———. 1984, A&A, 132, 168
Chung, S.-J., et al. 2005, ApJ, 630, 535
Dominik, M. 1999, A&A, 349, 108
Dong, S., et al. 2008, ApJ, submitted (arXiv:0804.1354)
Gaudi, B. S. 2008, in ASP Conf. Ser. 398, Extreme Solar Systems, ed. D. Fischer et al. (San Francisco: ASP), 479
Gaudi, B. S., et al. 2007, Science, 319, 927
Gould, A.. 2008, preprint (arXiv:0803.4324)
Gould, A., & Loeb, A. 1992, ApJ, 396, 104
Gould, A., et al. 2006, ApJ, 644, L37
Griest, K., & Safizadeh, N. 1998, ApJ, 500, 37
Soszyński, I., et al. 2001, ApJ, 552, 731
Udalski, A., et al. 2005, ApJ, 628, L109
Witt, H. J. 1990, A&A, 236, 311
Yoo, J., et al. 2004, ApJ, 616, 1204